Environmental Science and Technology, Volume 56, Issue 18, September 2022, pp. 13245-13253
DOI:10.1021/acs.est.2c04727

Paper Device Combining CRISPR/Cas12a and RT-LAMP for SARS-CoV-2 Detection in Wastewater

Haorui Cao[a,b], Kang Mao[a*], Fang Ran[a], Pengqi Xu[c], Yirong Zhao[a,b], Xiangyan Zhang[d], Hourong Zhou[d,e], Zhugen Yang[f*], Hua Zhang[a*], and Guibin Jiang[g]

[a] *State Key Laboratory of Environmental Geochemistry, Institute of Geochemistry, Chinese Academy of Sciences, Guiyang, 550081, China*

[b] *University of Chinese Academy of Sciences, Beijing 100049, China.*

[c] *Precision Medicine Center, The Seventh Affiliated Hospital, Sun Yat-sen University, Shenzhen, 518107, China*

[d] *Guizhou Provincial People's Hospital, Guiyang, 550002, China.*

[e] *Jiangjunshan Hospital of Guizhou Province, Guiyang, 550001, China*

[f] *School of Water, Energy and Environment, Cranfield University, Cranfield, MK43 0AL, UK*

[g] *State Key Laboratory of Environmental Chemistry and Ecotoxicology, Research Center for Eco-Environmental Sciences, Chinese Academy of Sciences, Beijing 100085, China*

Corresponding Email: zhanghua@mail.gyig.ac.cn (Prof H. Zhang), maokang@mail.gyig.ac.cn

(Dr K. Mao), and zhugen.yang@cranfield.ac.uk (Dr Z. Yang)

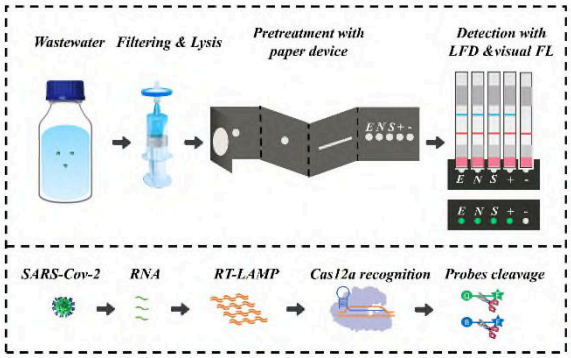

Graphical abstract

Abstract: Wastewater-based-surveillance of the COVID-19 pandemic holds great promise; however, a point-of-use detection method for SARS-CoV-2 in wastewater is lacking. Here, a portable paper device based on CRISPR/Cas12a and reverse-transcription loop-mediated isothermal amplification (RT-LAMP) with excellent sensitivity and specificity was developed for SARS-CoV-2 detection in wastewater. Three primer sets of RT-LAMP and guide RNAs (gRNAs) that could lead Cas12a to recognize target genes via base pairing were used to perform the high-fidelity RT-LAMP to detect the N, E, and S genes of SARS-CoV-2. Due to the trans-cleavage activity of CRISPR/Cas12a after high-fidelity amplicon recognition, carboxyfluorescein-ssDNA-Black Hole Quencher-1 and carboxyfluorescein-ssDNA-biotin probes were adopted to realize different visualization pathways via a fluorescence or lateral flow analysis, respectively. The reactions were integrated into a paper device for simultaneously detecting the N, E, and S genes with limits of detection (LODs) of 25, 310, and 10 copies/mL, respectively. The device achieved a semiquantitative analysis from 0-310 copies/mL due to the different LODs of the three genes. Blind experiments demonstrated that the device was suitable for wastewater analysis with 97.7% sensitivity and 82% semiquantitative accuracy. This is the first semiquantitative endpoint detection of SARS-CoV-2 in wastewater via different LODs, demonstrating a promising point-of-use method for wastewater-based-surveillance.

Keywords: SARS-CoV-2, CRISPR/Cas12a, RT-LAMP, Paper device, Wastewater

Published by ACS. This is the Author Accepted Manuscript issued with: Creative Commons Attribution Non-Commercial License (CC:BY:NC 4.0).
The final published version (version of record) is available online at DOI:10.1021/acs.est.2c04727. Please refer to any applicable publisher terms of use.

Synopsis: This study reports a novel integrated paper device based on CRISPR/Cas12a and reverse transcription loop-mediated isothermal amplification for the detection of SARS-CoV-2 in wastewater, providing a potential point-of-use tool for wastewater surveillance.

1. Introduction

The outbreak of the coronavirus disease 2019 (COVID-19) pandemic caused by severe acute respiratory syndrome coronavirus 2 (SARS-CoV-2) has resulted in nearly 0.5 billion confirmed cases and over 6 million deaths as of June 1, 2022, triggering a global public health crisis and bringing unprecedented challenges to the public health system [1-3]. The efficient surveillance and management of COVID-19 are critical for alleviating and preventing pandemics due to the high transmission efficiency and various potential spread routes, such as airborne, droplet, and fomite transmissions [4, 5]. As an alternative, wastewater-based-surveillance (WBS) is an efficient approach with great potential for warning of infectious disease outbreaks and transmission [6, 7]. Accordingly, in March 2020, we also proposed that a wastewater analysis can be used for the surveillance of the COVID-19 pandemic [8]. Subsequently, SARS-CoV-2 has been successfully detected in wastewater in many countries, including America, India, China, Canada and some European countries [9-11]. Therefore, Bivens et al. appealed for global collaboration to maximize contributions in the fight against COVID-19 with WBS [12].

However, the use of the WBS approach for developing a warning system and consequent effective intervention system requires a rapid analytical method for the on-site detection of SARS-CoV-2 in wastewater collection points. Currently, the most

commonly used analytical methods for SARS-CoV-2 detection are RT–qPCR, serological assays and paper-based sensors, such as lateral flow kits [13-15]. RT–qPCR requires expensive instruments, sophisticated operations and professionals to conduct the experiment for more than 6 hours, limiting its field use [16]. Although serological methods can be completed in a short time and require no complicated equipment, their low sensitivity to mild and asymptomatic infections and long time to produce an antibody response restrict their utilization in WBS [17, 18]. Herein, lateral flow kits developed via serological methods are also not suitable for WBS. Therefore, it is critical to develop a novel point-of-use (POU) method for SARS-CoV-2 detection in wastewater for the surveillance of the pandemic.

Isothermal amplifications, such as loop-mediated isothermal amplification (LAMP) and rolling circle amplification, are potential POU methods due to their high amplification efficiency, excellent specificity and low dependency on complicated thermal cycling equipment [19]. Among these isothermal amplification reactions, LAMP is a constant temperature reaction carried out between 60-65°C; the reaction is also much faster than other approaches and can be finished in less than one hour [20-23]. LAMP adopts six primers to bind eight regions of target DNA, and then, the reaction is started by the loop structure and DNA polymerase with a strand displacement function, while RT-LAMP requires the additional step to convert RNA into DNA by reverse transcriptase before conducting the LAMP reaction [24, 25]. Due to its obvious advantages, it has already been applied to the detection of various pathogens. For instance, Urrutia-Cabrera et al utilized the method to detect ORF1ab RdRP, ORF1ab nsp3 and N gene

fragments of SARS-CoV-2. The reaction could be finished in 30 min, and the limit of detection (LOD) reached 100 copies/μL [26]. However, false positives, which may be caused by primer-dimers, off-target hybrids, etc. appearing in the amplification of ORF1ab RdRP and ORF1ab nsp3, negatively affect the reliability of the method. Similarly, this issue was present in Suleman et al.'s study, which utilized LAMP to detect Toxoplasma gondii [27]. Because there were no denaturation and annealing steps at each cycle, the method suffered from nonignorable shortcomings, such as false positives, more frequently than PCR, especially in POU detection, where nonspecific dyes, such as calcein, are usually used as reaction indicators [28-30].

Recently, much more attention has been given to the use of CRISPR/Cas-based gene editing for further improvement of the specificity of analytical methods [31]. Due to the high-fidelity recognition of CRISPR/Cas technology from its single-base resolution and its powerful and flexible signal transduction ability due to efficient trans-cleavage, it has become a promising detection method [32, 33]. However, the sensitivity of CRISPR/Cas does not appear to be sufficient [34]. Some studies have attempted to combine CRISPR/Cas with isothermal amplification, utilizing the specificity of CRISPR/Cas to solve the false positive problem of isothermal amplification and using the high sensitivity of isothermal amplification to improve the LOD of CRISPR/Cas [32, 35]. Cas12a-RT-LAMP is a representative combination reaction and has already been used for SARS-CoV-2 detection [16, 22]. Broughton et al developed a lateral flow assay based on combination of Cas12a and RT-LAMP and could detect as low as 10 copies/μL in a clinical sample [16]. Utilizing the characteristic of FAM,

which can be excited to release green fluorescence under blue light, Wang et al and Pang et al established a visual detection method and integrated the Cas12a trans-cleavage reaction and isothermal amplification into one tube by building two temperature regions in one device [35, 36]. However, to date, the combination of Cas12a and RT-LAMP is still mainly used in clinical sample testing. Due to the large differences between wastewater samples and clinical samples, including a much lower virus concentration caused by dilution and more complicated matrix giving rise to various sources, whether the sensitivity and specificity of the reaction are enough for WBS remains unclear.

In this paper, a novel paper device combining RT-LAMP with Cas12a was developed and successfully applied to wastewater analysis. The wastewater samples were first enriched by filtration, followed by lysis on a microporous membrane. Then, the lysate was introduced to the paper device for RNA purification and allocation into reaction chambers. The high-fidelity RT-LAMP (HF-RT-LAMP) reaction was performed to detect three specific gene fragments, N, E, and S, which are current widely used target genes in RT–qPCR testing for SARS-CoV-2. The results could be read by the naked eye after excitation by 480 nm light or lateral flow dipsticks. The design and composition of the device are demonstrated in Fig 1 and Fig S2. Then, wastewater spiked with SARS-CoV-2 was utilized to assess the LODs and quantitative ability of the device. Blind testing was further applied to verify its reliability. Finally, the method was applied to wastewater monitoring in the city of Guiyang, China to help in the prevention and control of the SARS-CoV-2 pandemic.

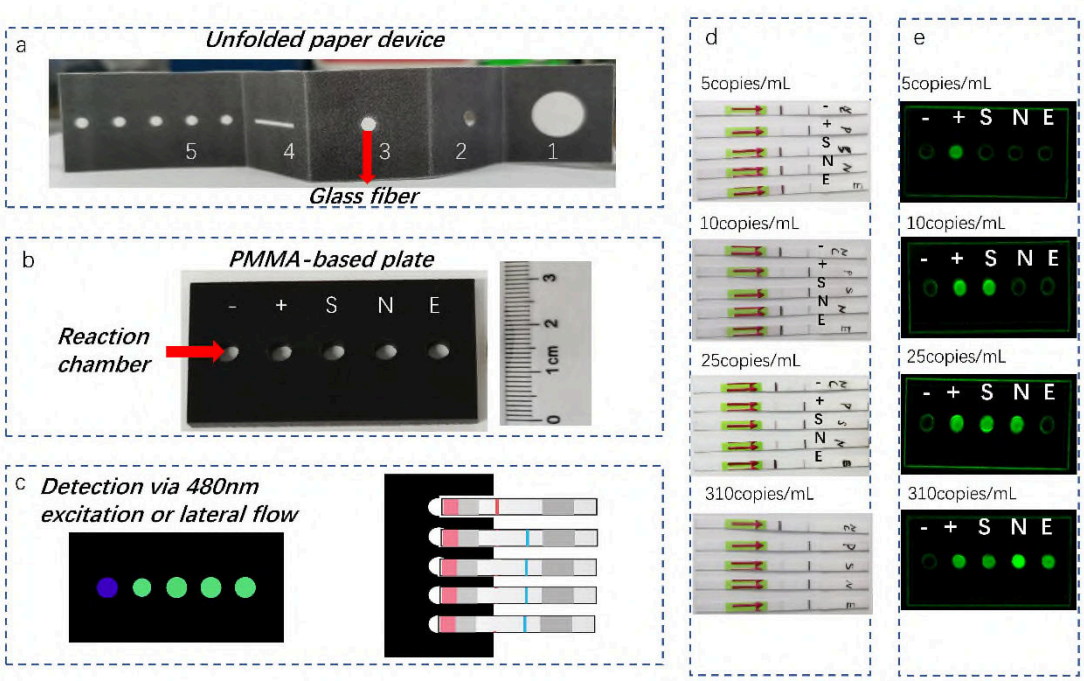

Fig. 1. Design and usage of the paper device for the detection of N, E, and S gene fragments with internal negative and positive controls. (a) The paper chip consisted of five parts labeled 1 to 5. Part 1 was composed of a large hydrophilicity disc surrounded by a wax-printed hydrophobic region. Part 2 utilized a small hole generated by a puncher for liquid transport. Part 3 consisted of a glass fiber disc for RNA-specific adsorption and a wax-printed region for liquid constraint. Part 4 utilized a rectangle channel for the allocation of elution buffer into three small hydrophilicity paper discs in Part 5. Part 5 consisted of three paper discs for sample RNA loading and two paper discs for negative and positive controls. (b) Polymethyl methacrylate (PMMA) plate for the LAMP reaction and Cas12a detection. (c) The results could be read by 480 nm excitation or a lateral flow strip. (d) Detection results of the paper device based on the lateral flow method. (e) Detection results of the paper device based on the fluorescence method. The black microfluidic plate can be changed to transparent if the light is blocked.

2. Materials and Methods

2.1 In vitro transcription

N, E, and S RNA fragments were generated by in vitro transcription. First, PCR was conducted on the plasmid (for the generation of the N and E gene transcription template, plasmid SARS-CoV-2-5 purchased from Genewiz (USA) was used, and for the S gene, plasmid 2019-nCoV S purchased from Sangon Biotech was adopted) with a forward primer containing the T7 promotor at the 5' end and a normal reverse primer to obtain enough transcription template. Then, the product was purified and condensed by gel recovery. Next, 0.5 μg purified product was used as a template for in vitro transcription according to the instructions of the HiScribe T7 Quick High Yield RNA Synthesis Kit. The products were purified by VAHTS RNA Clean Beads, and the DNA template was digested by DNase I. Finally, the concentration of RNA was determined by a Qubit 4.0 fluorometer, and the RNA was stored in a -80°C refrigerator.

2.2 RT-LAMP for SARS-CoV-2 assay

The RT-LAMP reaction adopted a 20 μL system, containing 0.1 μM outer primers F3/B3, 0.8 μM inner primers FIP/BIP, 0.6 μM loop primers LF/LB, 10 μL NEB WarmStart LAMP 2X Master Mix, 2 μL sample, 1 μL 20× Evagreen, and 4 μL DNase/RNase-Free distilled water. The reaction was incubated at 65°C for 30 min, and the fluorescence intensity was read by an ABI7500 system (Thermo Fisher Scientific (USA)). Then, 10 μL amplicons were utilized for agarose gel electrophoresis to verify the product.

2.3 Construction of HF-RT-LAMP for SARS-CoV-2

HF-RT-LAMP consists of an RT-LAMP reaction and subsequent CRISPR/Cas12a detection. The RT-LAMP reaction was similar to that described in Section 2.4, except for no Evagreen was added to the HF-RT-LAMP system. First, 18 μL Cas12a cleavage premix containing 100 nM Cas12a, 125 nM gRNA, and 500 nM fluorescent probe in 1× NEBuffer2.1 were incubated at 37°C for 10 min, followed by the addition of 2 μL RT-LAMP amplicons. Then, the reaction was incubated at 37°C for 30 min, and the fluorescence intensity was read by an ABI7500 system.

2.4 Visualization of HF-RT-LAMP for SARS-CoV-2

The visualization based on fluorescence was similar to that described in Section 2.5. After incubation of the cleavage reaction, 480 nm blue light was used to excite the solution. Then, the solution releases light green fluorescence that can be observed by the naked eye in the presence of targets, while no color can be observed under negative conditions. The color information was extracted by ImageJ.

For the lateral flow analysis, the fluorescent probe was replaced by lateral flow probes, while the other components were similar to those in the fluorescence method. First, 2 μL amplicons were added to 18 μL of premix, and then, 30 μL 1× NEBuffer 2.1 were added; the reaction was incubated at 37°C for 30 min, followed by inserting a test strip (Milenia HybriDetect 1, TwistDx UK) into the reaction tube. Next, a negative or positive result was distinguished based on the position of the strip. The color

information of the strip can also be extracted by ImageJ.

2.5 Wastewater samples collection and detection

Influent wastewater samples were collected from wastewater treatment plants (Erqiao (106.6776°E, 26.5696°N) and Jinyang (106.6439°E, 26.5948°N)) from June to November 2021 once a month. The wastewater samples were concentrated by a microporous filter adsorption method. First, a 0.22 μm microporous filter was used to remove large particles, and then, the pH was adjusted to ≈7 by 1 M HCl and 1 M NaOH with the help of a portable pH meter, followed by adding Mg^{2+} to 25 mM via 1 M $MgCl_2$ and the volume needed to be adjusted according to the initial concentration. The initial concentration of Mg^{2+} was detected via a commercial calcium and magnesium hardness tester. Next, 10 mL of the solution were filtered by a 0.22 μm microporous filter. Then, 40 μL GuSCN lysis solution were added to the microporous filter to break the virus for approximately 5 min at 37°C. Then, the lysis buffer was transferred to the paper device for RNA purification and the HF-RT-LAMP reaction. The device consisted of a PMMA plate, which was used as reaction chamber, a paper chip containing wax-printed filter paper, which was utilized to construct microfluidic channels, and a glass fiber disc, which could specifically absorb RNA (Fig. 1 and Fig. S2). As shown in Fig. 4, pure RNA could be obtained by the folded paper chip and directly applied to the HF-RT-LAMP reaction, while impurities, such as proteins and small molecules that may interfere with the amplification reaction, could be thoroughly removed. The detailed operations are shown in the SI Movie. For each test, a positive control and a negative

control were performed to ensure that the analysis worked normally and that there were no contaminations. The negative control was a blank water sample, and the positive control was sewage water dosed with 1000 copies/mL inactivated SARS-CoV-2 virus. The inactivated SARS-CoV-2 virus was obtained from Jiangjunshan Hospital in Guizhou Province, China.

3. Results and Discussion

3.1 Principle of HF-RT-LAMP

The principle of HF-RT-LAMP is shown in Scheme 1. First, three sets of primers targeting N, E, and S gene fragments were utilized to perform reverse transcription amplification of the three genes, resulting in many amplicons. Next, the Cas12a-gRNA complex recognizes the amplicons but is activated only when the amplicons are the target products. The ssDNA probes are cleaved due to trans-cleavage after the activation of the Cas12a-gRNA complex. The fluorescent probes are modified with a FAM group and its quenching group BHQ1. The quenching group and the fluorescent group are separated after cleavage, and light green fluorescence is observable after excitation by 480 nm light.

For the lateral flow probes, FAM and biotin were separately modified on both sides of ssDNA. As shown in Scheme 1 and Fig. S1, gold nanoparticles (GNPs) modified with gt anti FITC/FAM antibody are immobilized in the gray region, which is adjacent to the red region; the control line (red line) is modified with streptavidin, which can bind biotin; and the test line (blue line) is modified with anti-gt antibody, which can

bind gt antibody. The GNPs are immobilized at the control line due to the binding of biotin and streptavidin due to the lack of cleavage. In contrast, the GNPs are fixed at the test line due to the separation of GNPs and biotin and binding of the gt antibody and anti-gt antibody.

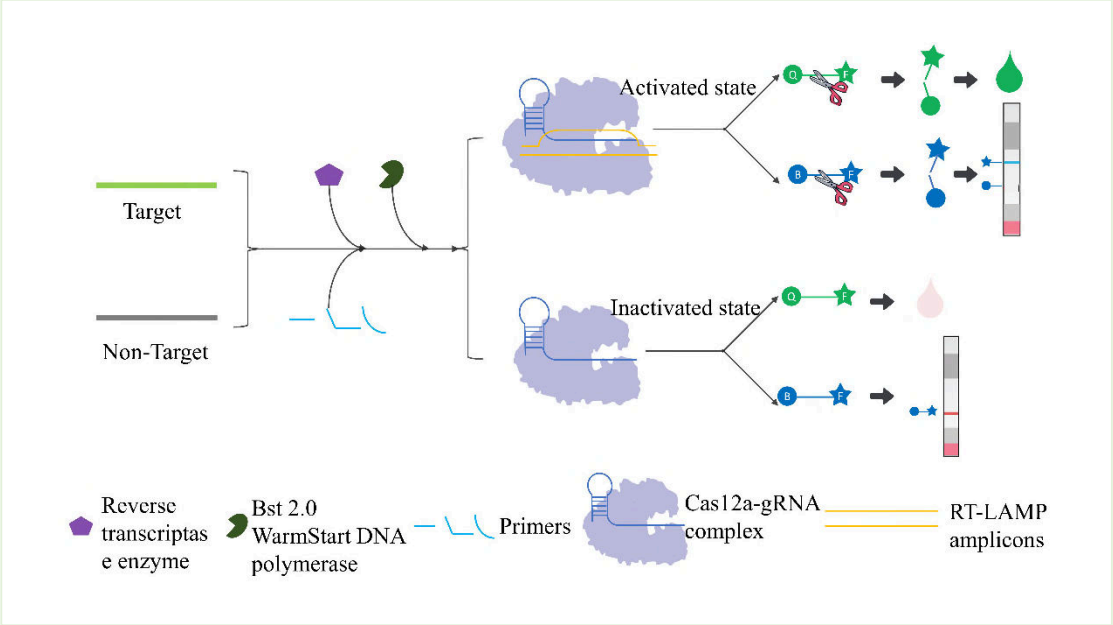

Scheme 1 Detection mechanisms of HF-RT-LAMP. In the presence of SARS-CoV-2, quantities of amplicons are generated via RT-LAMP, which could activate the trans-cleavage of the Cas12a-gRNA complex. Then, the complex unspecifically and readily cleaves ssDNA probes. Fluorescence is generated due to the separation of the fluorophore (FAM) and quencher (BHQ1) in the fluorescence method. In the lateral flow method, a strong test-stained band is produced due to the separation of FAM and biotin because the former could combine with modified gold nanoparticles and becomes immobilized on the test line, while the latter is fixed on the control line. However, in the absence of SARS-CoV-2, no amplicons are generated, and the Cas12a-gRNA complex cannot be activated. Therefore, the probes remain intact, and no fluorescence is observed due to the short distance between the quencher and fluorophore in the fluorescence method, while a slight test band

is observed with the probes that are mostly fixed on the control line due to their biotin groups.

3.2 Evaluation of RT-LAMP for SARS-CoV-2

RT-LAMP is the key step of the first target recognition and signal amplification of HF-RT-LAMP. Therefore, to better construct an HF-RT-LAMP system and compare the two methods, RT-LAMP was first established to detect the N, E, and S gene fragments of SARS-CoV-2. Target RNA generated by in vitro transcription was subjected to 10-fold serial dilution. Then, the dilution was utilized for LOD testing via real-time fluorescent RT-LAMP. Agarose gel electrophoresis was used to further verify the results. Ladder stripes were generated when the concentrations were higher or equal to the LODs because the specific amplicons of RT-LAMP are a mixture of various lengths and different structures, including stem–loop DNAs with various stem lengths and cauliflower-like structures with multiple loops.

As shown in Fig. 2 a-c, ladder stripes started to appear in lanes 4, 5, and 4 of the N, E, and S fractions, respectively, indicating that the method could detect the N, E and S genes at concentrations as low as 15, 260, and 5 copies/μL, respectively. The relationship between the lane numbers and target concentrations are demonstrated in the annotation of Fig. 2. We further analyzed more concentrations with narrow intervals to explore their LODs. The results showed that their LODs were 15, 260, and 3 copies/μL, respectively (Fig. S3). Their fluorescence intensity at the endpoint was further analyzed; however, no correlation was observed between the concentration and fluorescence intensity due to saturation of the reactions (Fig. 2 d-f), which could also

be confirmed by the fluorescence curves (Fig. S4). Therefore, RT-LAMP could not be used for endpoint quantitative analysis.

Then, whether real-time fluorescence can be used for quantitative analysis was confirmed. The fluorescence intensity was first normalized, with 0.25 chosen as the threshold. The time to the threshold exhibited a highly linear relationship with the logarithm of the concentration. The R^2 values exceeded 0.99, and for the E and S genes, the values were even higher than 0.999. Moreover, the linear range spanned 6-8 orders of magnitude, indicating that RT-LAMP has excellent real-time quantification capabilities (Fig. 2 g-i). However, considering the lack of real-time analysis equipment and that the qualitative results could also determine whether there were SARS-CoV-2 carriers, RT-LAMP was more suitable for endpoint qualitative analysis.

Notably, in terms of on-site qualitative testing, false positives caused by nonspecific amplification interfere with the test results [37]. As shown in Fig. 2 a-c, stripes appeared at the front end in lines 2-3, which were formed by small DNA fragments, indicating that there were dimers in the negative control and samples with concentrations below the LODs. Line 4 of b even presented stripes generated by serious nonspecific amplification, which was also confirmed by the fluorescence curves shown in Fig. S3. Although false positives could be distinguished by the shape and position of the electrophoretic stripes, nonspecific methods, such as calcein and turbidity assessment, which are often used in POU detection, cannot discriminate between false positives and true positives. To solve this issue, the CRISPR/Cas12a system was introduced to the subsequent reaction to construct an HF-RT-LAMP system.

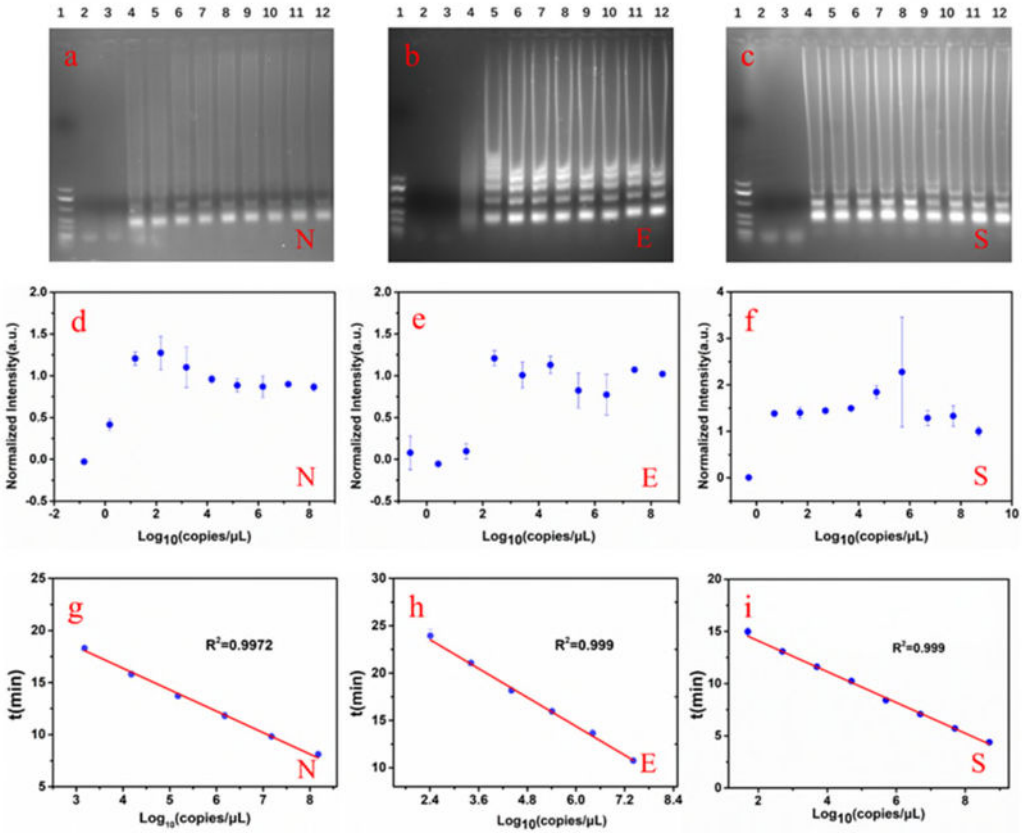

Fig. 2. RT-LAMP performance in the detection of N, E, and S gene fragments. a-c: Gel electrophoretic characterization of the N, E, and S gene amplicons. Lines 1 and 2 of a-c represent the marker and negative control, respectively, lines a3-12: $1.5x10^{0}$ to $1.5x10^{9}$ copies/μL according to a 10-fold increase; b3-12: $2.6x10^{0}$ to $2.6x10^{9}$ copies/μL according to a 10-fold increase; c3-12: $5x10^{-1}$ to $5x10^{8}$ copies/μL according to a 10-fold increase. d-f: Normalized intensity at the endpoint of the N, E, and S gene fragments; g-i; Quantitative curve of the N, E and S genes.

3.3 Construction and evaluation of HF-RT-LAMP

Due to the difference between nonspecific amplicons and the target amplicons, CRISPR/Cas12a was introduced to the reaction because it can recognize the sequence and eliminate the interference caused by nonspecific amplification. The gRNAs targeting amplification regions were selected to construct the Cas12a identification

system, which was then combined with RT-LAMP to establish HF-RT-LAMP analysis. The negative control and serial dilution were utilized to assess whether HF-RT-LAMP could solve the false positive issue and whether the introduction of Cas12a would affect the sensitivity.

As shown in Fig. 3 a-c and Fig. S3 d-f, the false positive issue was solved, but the LODs were not affected, indicating the precise identification capability and highly efficient signal transduction of HF-RT-LAMP. No fluorescence was observed in the negative control under blue light excitation, while the positive samples emitted green fluorescence. The fluorescence signal intensity could also be extracted by ImageJ, and the results were similar to those from naked-eye observation.

Then, the fluorescent probe was replaced by lateral flow probes to achieve lateral flow signal transduction. As shown in Fig. 3d-f, a slightly weak stripe may also appear in the test line in the negative test; with the help of ImageJ, it was easy to distinguish whether the band belonged to the positive or background signal. According to the gray data extracted from the negative sample via ImageJ, the threshold of the negative results at the test line was 172.2±15.6, while that of the positive results was approximately 40 to 70.

In general, the two visual methods did not differ, except for the modified groups of probes, indicating that HF-RT-LAMP has great flexibility and can easily meet the requirement of different sites. The fluorescence analysis was easier to perform but needed a portable illumination system for excitation at 480 nm, while the lateral flow analysis was slightly more complicated but enabled direct observation. Thus, the

fluorescence method is more suitable for locations with an available illumination system, while the lateral flow assay is more appropriate for sites without a similar instrument.

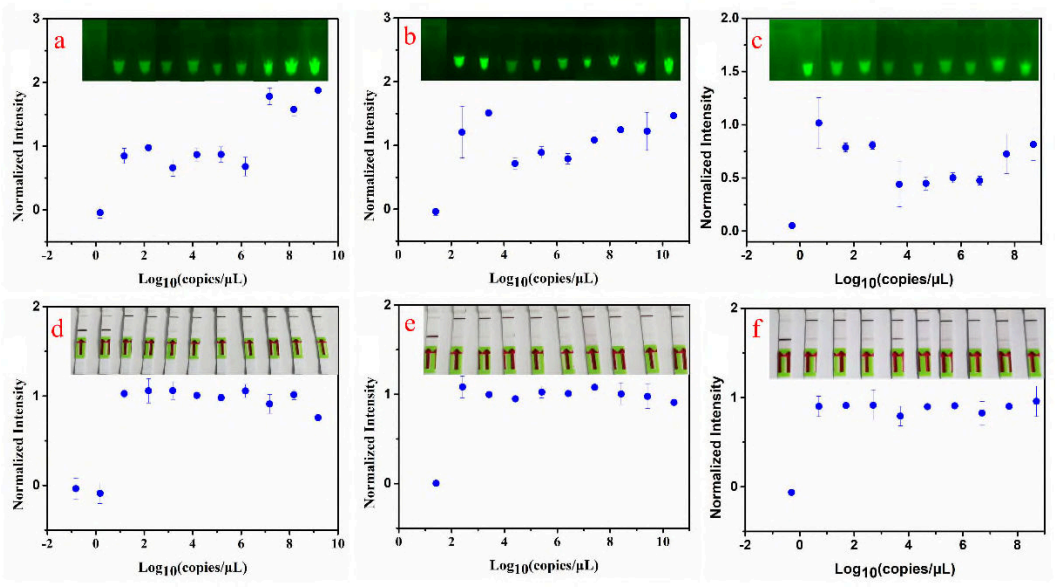

Fig. 3. Visualization of HF-RT-LAMP and the normalized intensity extracted via ImageJ. a-c: Visualization and normalization based on fluorescence signals. d-f: Visualization and normalization based on lateral flow signals. The lateral flow signal intensity was multiplied by minus one before normalization.

3.4. Construction of the paper device

Although HF-RT-LAMP possesses high sensitivity, strong specificity and flexible signal transduction ability with no need for complicated instrumentation, the complicated pretreatment (including lysis, extraction, enrichment and purification) steps with precise equipment limits further on-site analysis of SARS-CoV-2 in complicated wastewater. Thus, a paper device was introduced to overcome this issue.

Then, wastewater spiked with different amounts of SARS-CoV-2 virus was

adopted to evaluate the detection performance of the paper device. As shown in Fig. S5, the LODs of the S, N, and E gene fragments reached 10, 25, and 310 copies/mL, respectively, and no false positives were observed. According to Wu et al's research, the virus titers in wastewater during the pandemic were usually between 10^1 and 10^3 copies/ml [38]. Hence, the integrated device holds great potential for the surveillance of SARS-CoV-2 in wastewater. Considering the enrichment efficiency, lysis performance, degradation of RNA and allocation of samples in which one sample was divided into three, the sensitivity was not significantly decreased. Therefore, the paper device had a limited impact on the method, indicating the great compatibility between HF-RT-LAMP and the paper device.

More importantly, the device successfully overcame the quantitative problem of endpoint detection. Due to the different LODs of the N, E, and S gene fragments, the fabricated device possessed a semiquantitative ability from 0-310 copies/mL (Fig. 1e). Three channels were all negative when the concentration of the virus in wastewater was lower than 10 copies/mL, indicating that the community was in a low-risk state (Fig. 1e and Fig. S5). When the concentration was between 10 and 25 copies/mL, the S gene channel was positive, while the other channels were negative, suggesting that the community had a medium risk and that the virus started to spread (Fig. 1e and Fig. S5). The N and S channels were positive when the virus content was higher than 25 copies/mL but lower than 310 copies/mL, indicating that the community was in a high-risk state (Fig. 1e and Fig. S5). All channels were positive if the concentration exceeded 310 copies/mL, indicating that the community had an extremely high risk and that the

virus spread widely (Fig. 1e and Fig. S5). The risk reflected by the novel device was similar to that in Wu et al's research [38].

Overall, the paper device not only ameliorated the problem of nucleic acid extraction and purification under on-site conditions but also achieved semiquantitative analysis with its multiplexed detection, realizing a revolutionary leap from rapid detection to rapid-precision visual risk assessment. This system also provides a new idea for semiquantitative POU analysis. Compared with other methods developed for the detection of SARS-CoV-2, this assay possessed extremely high sensitivity and extraordinary semiquantitative ability with four gradients (Table S3).

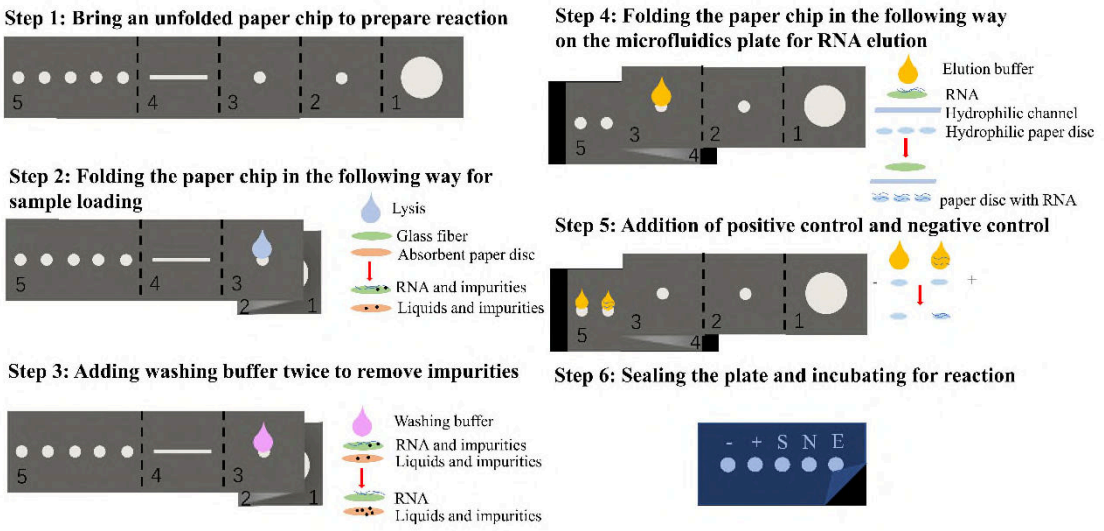

Fig. 4 Paper folding and plate sealing procedures for lysate loading, RNA washing, elution, and plate sealing for the reaction. Step 1: Preparing the reaction with an unfold paper consisted of a wax-printed filter paper composed of 5 parts and a glass fiber disc. Step 2: Folding the paper chip according to step 2 in the figure, followed by loading 40 μL lysis buffer onto the center of the glass fiber in Part 3. Step 3: After sample loading, 100 μL washing buffer was added to the glass fiber

disc in Part 3 to eliminate impurities. The washing step was conducted at least twice. Step 4: RNase-free water was added to dried glass fiber to elute RNA to the paper disc in Part 5. Step 5: RNase-free water was added to the negative control, and RNase-free water with SARS-CoV-2 RNA was added to the positive control. Step 6: Sealing the plate for incubation.

3.5 Wastewater monitoring and blind test

To further prove the reliability of the assay, a blind experiment was conducted. We spiked SARS-CoV-2 virus obtained from Jiangjunshan Hospital into wastewater. To better simulate community sewage at different stages of the pandemic, 50 samples with different concentrations from 0-500 copies/mL were prepared. Then, the samples were tested randomly by another group of experimenters who were blinded to the sample concentrations. As shown in Table S2 and Fig. S6, 43 of 44 wastewater samples spiked with SARS-CoV-2 were successfully detected, and no false positives appeared in the test, indicating that its sensitivity reached 97.7% and showing that the method could easily distinguish between negative and positive samples.

The excellent semiquantitative ability was also confirmed in the experiment as 41 of 50 semiquantitative results were consistent with their concentrations, indicating that the accuracy reached 82%. Only one sample was not detected due to its low concentration, while nine semiquantitative results were not in agreement with the actual values. Although a few semiquantitative results were not strictly accurate, the fabricated device still possesses excellent sensitivity, demonstrating its great potential in wastewater analysis. In the future, we aim to further optimize the method by adjusting

the reaction system and designing new primers to improve the accuracy of the semiquantitative results.

Finally, the device was applied to wastewater analysis for half a year from June to November in 2021 to further verify its performance. The Erqiao WWTP in Huaguoyuan, which is one of the largest communities in Asia, and Jinyang WWTP, which is located in a new urban area in Guiyang, were chosen as the target sites. Based on the results, no virus was detected in sewage during the six months, suggesting that the communities were in a low-risk state, which is similar to the findings of the Centers for Disease Control and Prevention (CDC). Thus, the novel device has excellent potential in sewage detection.

A portable multiplexed paper device based on a combination of CRISPR/Cas12a and RT-LAMP for POU detection of SARS-CoV-2 in wastewater was constructed in this study. The detection process takes less than 2 hours from sampling to results, without the need for any complicated equipment. Due to the high resolution and great signal transduction of Cas12a, this novel analytical method successfully overcame the false positive issue of RT-LAMP while realizing visual detection and can be used in resource-limited areas, such as WWTPs. The analytical performance did not significantly decrease after being integrated into the paper device due to the great compatibility between the paper device and the HF-RT-LAMP method. Furthermore, the multiplexing characteristics endowed the method with semiquantitative ability due to the difference in the LOD of the N, E, and S gene fragments, which reached 10, 25, and 310 copies/mL, respectively; thus, the device realized semiquantitative analysis

from 0-310 copies/mL. Wastewater verification and blind testing further demonstrated the reliability of the fabricated device, which possessed 97.7% sensitivity and 82% semiquantitative accuracy. In the future, the reaction system and primers will be optimized to further improve the semiquantitative accuracy. Therefore, the device not only rapidly detected the virus in sewage but also realized precise visual risk assessment, which also provides a new idea for endpoint semiquantitative analysis. Last but not least, the integrated device is universal, with only primers and gRNAs needing to be changed when used for other pathogens. Therefore, the fabricated paper device based on CRISPR/Cas12a and RT-LAMP holds great potential for wastewater-based-surveillance.

Supporting Information

The Supporting Information is available free of charge at https://pubs.acs.org

- List of primers and gRNA sequences; Results of blind tests of wastewater samples; Comparison of the developed method and other assays; Evaluation of limits of detection of the N, E, and S genes; Principle of lateral flow dipsticks; Design of the paper device; Normalized fluorescence intensity curve of RT-LAMP
- Movie describing the detailed operation processes of samples on the paper device file

Acknowledgment

The authors acknowledge the support from the National Key Research and Development Program of China (2020YFC1807300), the National Natural Science

Foundation of China (42107486), Guizhou Provincial Science and Technology Projects (Qiankehe Zhicheng [2020] 4Y190, Qiankehe Jichu-ZK [2022] Yiban 565), Youth Cross Team Project of CAS (JCTD-2021-17), and STS of CAS (KFJ-STS-QYZD-185). ZY thanks UK NERC Fellowship grant (NE/R013349/2) and N-WESP (NE/V010441/1). The authors would like to thank the Editor and all the anonymous reviewers for their constructive comments that significantly improved the quality of the manuscript.

References

1. Zhou, P.; Yang, X. L.; Wang, X. G.; Hu, B.; Zhang, L.; Zhang, W.; Si, H. R.; Zhu, Y.; Li, B.; Huang, C. L.; Chen, H. D.; Chen, J.; Luo, Y.; Guo, H.; Jiang, R. D.; Liu, M. Q.; Chen, Y.; Shen, X. R.; Wang, X.; Zheng, X. S.; Zhao, K.; Chen, Q. J.; Deng, F.; Liu, L. L.; Yan, B.; Zhan, F. X.; Wang, Y. Y.; Xiao, G. F.; Shi, Z. L., A pneumonia outbreak associated with a new coronavirus of probable bat origin. *Nature* **2020,** *579*, (7798), 270–273.

2. Grantz, K. H.; Meredith, H. R.; Cummings, D. A. T.; Metcalf, C. J. E.; Grenfell, B. T.; Giles, J. R.; Mehta, S.; Solomon, S.; Labrique, A.; Kishore, N.; Buckee, C. O.; Wesolowski, A., The use of mobile phone data to inform analysis of COVID-19 pandemic epidemiology. *Nat Commun* **2020,** *11*, (1), 4961.

3. Li, Z.; Song, G.; Bi, Y.; Gao, W.; He, A.; Lu, Y.; Wang, Y.; Jiang, G., Occurrence and Distribution of Disinfection Byproducts in Domestic Wastewater Effluent, Tap Water, and Surface Water during the SARS-CoV-2 Pandemic in China. *Environ Sci Technol* **2021,** *55*, (7), 4103-4114.

4. Qu, G.; Li, X.; Hu, L.; Jiang, G., An Imperative Need for Research on the Role of

Environmental Factors in Transmission of Novel Coronavirus (COVID-19). *Environ Sci Technol* **2020,** *54*, (7), 3730-3732.

5. Hu, L.; Gao, J.; Yao, L.; Zeng, L.; Liu, Q.; Zhou, Q.; Zhang, H.; Lu, D.; Fu, J.; Liu, Q. S.; Li, M.; Zhao, X.; Hou, X.; Shi, J.; Liu, L.; Guo, Y.; Wang, Y.; Ying, G. G.; Cai, Y.; Yao, M.; Cai, Z.; Wu, Y.; Qu, G.; Jiang, G., Evidence of Foodborne Transmission of the Coronavirus (COVID-19) through the Animal Products Food Supply Chain. *Environ Sci Technol* **2021,** *55*, (5), 2713-2716.

6. McClary-Gutierrez, J. S.; Mattioli, M. C.; Marcenac, P.; Silverman, A. I.; Boehm, A. B.; Bibby, K.; Balliet, M.; de Los Reyes, F. L., 3rd; Gerrity, D.; Griffith, J. F.; Holden, P. A.; Katehis, D.; Kester, G.; LaCross, N.; Lipp, E. K.; Meiman, J.; Noble, R. T.; Brossard, D.; McLellan, S. L., SARS-CoV-2 Wastewater Surveillance for Public Health Action. *Emerg Infect Dis* **2021,** *27*, (9), 1-8.

7. Hughes, B.; Duong, D.; White, B. J.; Wigginton, K. R.; Chan, E. M. G.; Wolfe, M. K.; Boehm, A. B., Respiratory Syncytial Virus (RSV) RNA in Wastewater Settled Solids Reflects RSV Clinical Positivity Rates. *Environ. Sci. Technol. Lett.* **2022,** *9*, (2), 173-178.

8. Mao, K.; Zhang, H.; Yang, Z., Can a Paper-Based Device Trace COVID-19 Sources with Wastewater-Based Epidemiology? *Environ Sci Technol* **2020,** *54*, (7), 3733-3735.

9. Ali, W.; Zhang, H.; Wang, Z.; Chang, C.; Javed, A.; Ali, K.; Du, W.; Niazi, N. K.; Mao, K.; Yang, Z., Occurrence of various viruses and recent evidence of SARS-CoV-2 in wastewater systems. *J Hazard Mater* **2021,** *414*, 125439.

10. Korfmacher, K. S.; Harris-Lovett, S.; Nelson, K. L., Campus Collaborations As a Model for Transforming SARS-CoV-2 Wastewater Surveillance Research into Public Health Action.

Environ Sci Technol **2021,** *55*, (19), 12770-12772.

11. Kim, S.; Kennedy, L. C.; Wolfe, M. K.; Criddle, C. S.; Duong, D. H.; Topol, A.; White, B. J.; Kantor, R. S.; Nelson, K. L.; Steele, J. A.; Langlois, K.; Griffith, J. F.; Zimmer-Faust, A. G.; McLellan, S. L.; Schussman, M. K.; Ammerman, M.; Wigginton, K. R.; Bakker, K. M.; Boehm, A. B., SARS-CoV-2 RNA is enriched by orders of magnitude in primary settled solids relative to liquid wastewater at publicly owned treatment works. *Environ Sci (Camb)* **2022,** *8*, (4), 757-770.

12. Bivins, A.; North, D.; Ahmad, A.; Ahmed, W.; Alm, E.; Been, F.; Bhattacharya, P.; Bijlsma, L.; Boehm, A. B.; Brown, J.; Buttiglieri, G.; Calabro, V.; Carducci, A.; Castiglioni, S.; Cetecioglu Gurol, Z.; Chakraborty, S.; Costa, F.; Curcio, S.; de Los Reyes, F. L., 3rd; Delgado Vela, J.; Farkas, K.; Fernandez-Casi, X.; Gerba, C.; Gerrity, D.; Girones, R.; Gonzalez, R.; Haramoto, E.; Harris, A.; Holden, P. A.; Islam, M. T.; Jones, D. L.; Kasprzyk-Hordern, B.; Kitajima, M.; Kotlarz, N.; Kumar, M.; Kuroda, K.; La Rosa, G.; Malpei, F.; Mautus, M.; McLellan, S. L.; Medema, G.; Meschke, J. S.; Mueller, J.; Newton, R. J.; Nilsson, D.; Noble, R. T.; van Nuijs, A.; Peccia, J.; Perkins, T. A.; Pickering, A. J.; Rose, J.; Sanchez, G.; Smith, A.; Stadler, L.; Stauber, C.; Thomas, K.; van der Voorn, T.; Wigginton, K.; Zhu, K.; Bibby, K., Wastewater-Based Epidemiology: Global Collaborative to Maximize Contributions in the Fight Against COVID-19. *Environ Sci Technol* **2020,** *54*, (13), 7754-7757.

13. Vogels, C. B. F.; Brito, A. F.; Wyllie, A. L.; Fauver, J. R.; Ott, I. M.; Kalinich, C. C.; Petrone, M. E.; Casanovas-Massana, A.; Catherine Muenker, M.; Moore, A. J.; Klein, J.; Lu, P.; Lu-Culligan, A.; Jiang, X.; Kim, D. J.; Kudo, E.; Mao, T.; Moriyama, M.; Oh, J. E.; Park, A.; Silva, J.; Song, E.; Takahashi, T.; Taura, M.; Tokuyama, M.; Venkataraman, A.; Weizman, O. E.; Wong,

P.; Yang, Y.; Cheemarla, N. R.; White, E. B.; Lapidus, S.; Earnest, R.; Geng, B.; Vijayakumar, P.; Odio, C.; Fournier, J.; Bermejo, S.; Farhadian, S.; Dela Cruz, C. S.; Iwasaki, A.; Ko, A. I.; Landry, M. L.; Foxman, E. F.; Grubaugh, N. D., Analytical sensitivity and efficiency comparisons of SARS-CoV-2 RT-qPCR primer-probe sets. *Nat Microbiol* **2020,** *5*, (10), 1299-1305.

14. Cady, N. C.; Tokranova, N.; Minor, A.; Nikvand, N.; Strle, K.; Lee, W. T.; Page, W.; Guignon, E.; Pilar, A.; Gibson, G. N., Multiplexed detection and quantification of human antibody response to COVID-19 infection using a plasmon enhanced biosensor platform. *Biosens Bioelectron* **2021,** *171*, 112679.

15. Hu, R. B.; Liao, T.; Ren, Y.; Liu, W. M.; Ma, R.; Wang, X. Y.; Lin, Q. H.; Wang, G. X.; Liang, Y. Y., Sensitively detecting antigen of SARS-CoV-2 by NIR-II fluorescent nanoparticles. *Nano Res.* **2022,** *15*, (8), 7313–7319.

16. Broughton, J. P.; Deng, X.; Yu, G.; Fasching, C. L.; Servellita, V.; Singh, J.; Miao, X.; Streithorst, J. A.; Granados, A.; Sotomayor-Gonzalez, A.; Zorn, K.; Gopez, A.; Hsu, E.; Gu, W.; Miller, S.; Pan, C. Y.; Guevara, H.; Wadford, D. A.; Chen, J. S.; Chiu, C. Y., CRISPR-Cas12-based detection of SARS-CoV-2. *Nat Biotechnol* **2020,** *38*, (7), 870-874.

17. Liu, Z. L.; Liu, Y.; Wan, L. G.; Xiang, T. X.; Le, A. P.; Liu, P.; Peiris, M.; Poon, L. L. M.; Zhang, W., Antibody Profiles in Mild and Severe Cases of COVID-19. *Clin Chem* **2020,** *66*, (8), 1102-1104.

18. Sakthivel, D.; Delgado-Diaz, D.; McArthur, L.; Hopper, W.; Richards, J. S.; Narh, C. A., Point-of-Care Diagnostic Tools for Surveillance of SARS-CoV-2 Infections. *Front. Public Health* **2021,** *9*, 766871.

19. Zhao, Y.; Chen, F.; Li, Q.; Wang, L.; Fan, C., Isothermal Amplification of Nucleic Acids. *Chem Rev* **2015,** *115*, (22), 12491-545.

20. Chen, Y.; Shi, Y.; Chen, Y.; Yang, Z.; Wu, H.; Zhou, Z.; Li, J.; Ping, J.; He, L.; Shen, H.; Chen, Z.; Wu, J.; Yu, Y.; Zhang, Y.; Chen, H., Contamination-free visual detection of SARS-CoV-2 with CRISPR/Cas12a: A promising method in the point-of-care detection. *Biosens Bioelectron* **2020,** *169*, 112642.

21. Ji, T.; Liu, Z.; Wang, G.; Guo, X.; Akbar Khan, S.; Lai, C.; Chen, H.; Huang, S.; Xia, S.; Chen, B.; Jia, H.; Chen, Y.; Zhou, Q., Detection of COVID-19: A review of the current literature and future perspectives. *Biosens Bioelectron* **2020,** *166*, 112455.

22. Zhao, Y.; Fang, X.; Yu, H.; Fu, Y.; Zhao, Y., Universal Exponential Amplification Confers Multilocus Detection of Mutation-Prone Virus. *Anal. Chem.* **2022,** *94*, (2), 927-933.

23. Zhu, Y.; Wu, X.; Gu, A.; Dobelle, L.; Cid, C. A.; Li, J.; Hoffmann, M. R., Membrane-Based In-Gel Loop-Mediated Isothermal Amplification (mgLAMP) System for SARS-CoV-2 Quantification in Environmental Waters. *Environ Sci Technol* **2022,** *56*, (2), 862-873.

24. Rabe, B. A.; Cepko, C., SARS-CoV-2 detection using isothermal amplification and a rapid, inexpensive protocol for sample inactivation and purification. *Proc Natl Acad Sci U S A* **2020,** *117*, (39), 24450-24458.

25. Tomita, N.; Mori, Y.; Kanda, H.; Notomi, T., Loop-mediated isothermal amplification (LAMP) of gene sequences and simple visual detection of products. *Nat Protoc* **2008,** *3*, (5), 877-82.

26. Urrutia-Cabrera, D.; Liou, R. H.; Wang, J. H.; Chan, J.; Hung, S. S.; Hewitt, A. W.; Martin, K. R.; Edwards, T. L.; Kwan, P.; Wong, R. C., Comparative analysis of loop-mediated

isothermal amplification (LAMP)-based assays for rapid detection of SARS-CoV-2 genes. *Sci Rep* **2021,** *11*, (1), 22493.

27. Suleman, E.; Mtshali, M. S.; Lane, E., Investigation of false positives associated with loop-mediated isothermal amplification assays for detection of Toxoplasma gondii in archived tissue samples of captive felids. *J Vet Diagn Invest* **2016,** *28*, (5), 536-42.

28. Patchsung, M.; Jantarug, K.; Pattama, A.; Aphicho, K.; Suraritdechachai, S.; Meesawat, P.; Sappakhaw, K.; Leelahakorn, N.; Ruenkam, T.; Wongsatit, T.; Athipanyasilp, N.; Eiamthong, B.; Lakkanasirorat, B.; Phoodokmai, T.; Niljianskul, N.; Pakotiprapha, D.; Chanarat, S.; Homchan, A.; Tinikul, R.; Kamutira, P.; Phiwkaow, K.; Soithongcharoen, S.; Kantiwiriyawanitch, C.; Pongsupasa, V.; Trisrivirat, D.; Jaroensuk, J.; Wongnate, T.; Maenpuen, S.; Chaiyen, P.; Kamnerdnakta, S.; Swangsri, J.; Chuthapisith, S.; Sirivatanauksorn, Y.; Chaimayo, C.; Sutthent, R.; Kantakamalakul, W.; Joung, J.; Ladha, A.; Jin, X.; Gootenberg, J. S.; Abudayyeh, O. O.; Zhang, F.; Horthongkham, N.; Uttamapinant, C., Clinical validation of a Cas13-based assay for the detection of SARS-CoV-2 RNA. *Nat Biomed Eng* **2020,** *4*, (12), 1140-1149.

29. Becherer, L.; Borst, N.; Bakheit, M.; Frischmann, S.; Zengerle, R.; von Stetten, F., Loop-mediated isothermal amplification (LAMP) – review and classification of methods for sequence-specific detection. *Analytical Methods* **2020,** *12*, (6), 717-746.

30. Wang, Y.; Liu, D.; Deng, J.; Wang, Y.; Xu, J.; Ye, C., Loop-mediated isothermal amplification using self-avoiding molecular recognition systems and antarctic thermal sensitive uracil-DNA-glycosylase for detection of nucleic acid with prevention of carryover contamination. *Anal Chim Acta* **2017,** *996*, 74-87.

31. Li, Y.; Li, S.; Wang, J.; Liu, G., CRISPR/Cas Systems towards Next-Generation Biosensing. *Trends Biotechnol* **2019,** *37*, (7), 730-743.

32. Chen, J. S.; Ma, E.; Harrington, L. B.; Da Costa, M.; Tian, X.; Palefsky, J. M.; Doudna, J. A. J. e., CRISPR-Cas12a target binding unleashes indiscriminate single-stranded DNase activity. *Science* **2018,** *360*, (6387), 436-439.

33. Gootenberg, J. S.; Abudayyeh, O. O.; Kellner, M. J.; Joung, J.; Collins, J. J.; Zhang, F., Multiplexed and portable nucleic acid detection platform with Cas13, Cas12a, and Csm6. *Science* **2018,** *360*, (6387), 439-444.

34. Gootenberg, J. S.; Abudayyeh, O. O.; Lee, J. W.; Essletzbichler, P.; Dy, A. J.; Joung, J.; Verdine, V.; Donghia, N.; Daringer, N. M.; Freije, C. A.; Myhrvold, C.; Bhattacharyya, R. P.; Livny, J.; Regev, A.; Koonin, E. V.; Hung, D. T.; Sabeti, P. C.; Collins, J. J.; Zhang, F., Nucleic acid detection with CRISPR-Cas13a/C2c2. *Science* **2017,** *356*, (6336), 438-442.

35. Pang, B.; Xu, J.; Liu, Y.; Peng, H.; Feng, W.; Cao, Y.; Wu, J.; Xiao, H.; Pabbaraju, K.; Tipples, G.; Joyce, M. A.; Saffran, H. A.; Tyrrell, D. L.; Zhang, H.; Le, X. C., Isothermal Amplification and Ambient Visualization in a Single Tube for the Detection of SARS-CoV-2 Using Loop-Mediated Amplification and CRISPR Technology. *Anal Chem* **2020,** *92*, (24), 16204-16212.

36. Wang, R.; Qian, C.; Pang, Y.; Li, M.; Yang, Y.; Ma, H.; Zhao, M.; Qian, F.; Yu, H.; Liu, Z.; Ni, T.; Zheng, Y.; Wang, Y., opvCRISPR: One-pot visual RT-LAMP-CRISPR platform for SARS-cov-2 detection. *Biosens Bioelectron* **2021,** *172*, 112766.

37. Zhang, T.; Zhao, W.; Zhao, W.; Si, Y.; Chen, N.; Chen, X.; Zhang, X.; Fan, L.; Sui, G., Universally Stable and Precise CRISPR-LAMP Detection Platform for Precise Multiple

Respiratory Tract Virus Diagnosis Including Mutant SARS-CoV-2 Spike N501Y. *Anal. Chem.* **2021,** *93*, (48), 16184-16193.

38. Wu, F.; Xiao, A.; Zhang, J.; Moniz, K.; Endo, N.; Armas, F.; Bushman, M.; Chai, P. R.; Duvallet, C.; Erickson, T. B.; Foppe, K.; Ghaeli, N.; Gu, X.; Hanage, W. P.; Huang, K. H.; Lee, W. L.; McElroy, K. A.; Rhode, S. F.; Matus, M.; Wuertz, S.; Thompson, J.; Alm, E. J., Wastewater surveillance of SARS-CoV-2 across 40 U.S. states from February to June 2020. *Water Res* **2021,** *202*, 117400.

Cranfield University

CERES Research Repository **https://dspace.lib.cranfield.ac.uk/**

School of Water, Energy and Environment (SWEE) Staff publications (SWEE)

Paper device combining CRISPR/Cas12a and reverse-transcription loop-mediated isothermal amplification for SARS-CoV-2 detection in wastewater

Cao, Haorui

2022-08-30

Attribution-NonCommercial 4.0 International

Cao H, Mao K, Ran F, et al., (2022) Paper device combining CRISPR/Cas12a and reverse-transcription loop-mediated isothermal amplification for SARS-CoV-2 detection in wastewater. Environmental Science and Technology, Volume 56, Issue 18, September 2022, pp. 13245-13253

https://doi.org/10.1021/acs.est.2c04727

Downloaded from CERES Research Repository, Cranfield University